Available online at www.sciencedirect.com

ScienceDirect

ELSEVIER

Journal of Physics and Chemistry of Solids 68 (2007) 2293–2296

JOURNAL OF PHYSICS AND CHEMISTRY OF SOLIDS

www.elsevier.com/locate/jpcs

Properties of sol–gel dip-coated zinc oxide thin films

K.R. Murali*

Electrochemical Materials Science Division, Central Electrochemical Research Institute, Karaikudi 630 006, India

Received 11 February 2007; received in revised form 6 June 2007; accepted 21 June 2007

Abstract

Zinc oxide (ZnO) films were deposited on glass substrates by the sol–gel dip coating method using acrylamide route. The films were characterized by X-ray diffraction studies which indicated wurtzite structure. Optical absorption measurements indicated band gap in the range 3.17–3.32 eV. XPS studies indicated the formation of ZnO. The resistivity of the films were in the range 1000–10,000 ohm cm.
© 2007 Elsevier Ltd. All rights reserved.

Keywords: A. Oxides; A. Semiconductors; A. Thin films; B. Sol–gel growth

1. Introduction

Zinc oxide (ZnO) semiconductor films have been extensively investigated and have received considerable attention in recent years due to their interesting electro-optical properties, high electro-chemical stability, a large band gap, etc. ZnO is suitable for use in gas sensors [1,2], heat mirrors [3], transparent electrodes [4], solar cells [5–7] and piezoelectric devices [8]. ZnO films have been deposited by a number of methods like pulsed magnetron sputtering [9], electrodeposition process [10], sol–gel method [11], electrostatic spray deposition [12] and spray pyrolysis [4,13–18]. Among these methods, sol–gel dip coating method is a very simple process for the production of large area films. An earlier report on the preparation of ZnO by acrylamide route discusses the ZnO powder synthesis [11]. In this work, ZnO films were deposited by the acrylamide sol–gel dip coating method and their characteristics are reported.

2. Experimental methods

ZnO films were deposited on cleaned glass substrates from AR grade zinc chloride, acrylamide, bisacrylamide and ammonium persulphate. The pH of the zinc chloride solution was changed to 9 by adding AR grade ammonia solution. Acrylamide and bisacrylamide were then added to this solution. The temperature of the precursor mixture was kept at 70 °C. A small quantity of gelling agent ammonium persulphate was added till a viscous solution was obtained. The cleaned glass substrates (2.5×7.5 cm) were immersed in this solution and withdrawn at the rate of 1 cm/min. The deposit was then dried and finally post annealed at different temperatures in the range of 400–500 °C for different durations ranging from 60 to 240 min. The film thickness was determined gravimetrically [19], by measuring the change in weight of the substrate before and after film deposition, the area of deposition and using the bulk density of ZnO ($5.6\,g\,cm^{-3}$) and it was in the range 1.0–1.5 μm. Thicknesses of the films were also verified by Mutitoyo surface profilometer and it was found to be in the range 0.9–1.45 μm. The surface roughness measured by the surface profilometer was 2.34 nm.

3. Results and discussion

X-ray diffraction (XRD) experiments were performed using a PANalytical X-ray diffractometer. Cu K_α was used as the X-ray source. XRD spectra of the ZnO films heat treated at different temperatures is shown in Fig. 1. The standard XRD spectrum of ZnO powder (PDF80-0075) is also shown in the figure. All the films were *c*-axis oriented, i.e., the (0 0 2) axis was preferentially perpendicular to the surface of the substrate. Such *c*-axis oriented films are quite common for ZnO films grown at temperatures around

*Tel.: +91 4565227550; fax: +91 4565227553.
E-mail address: muraliramkrish@gmail.com

0022-3697/$ - see front matter © 2007 Elsevier Ltd. All rights reserved.
doi:10.1016/j.jpcs.2007.06.006

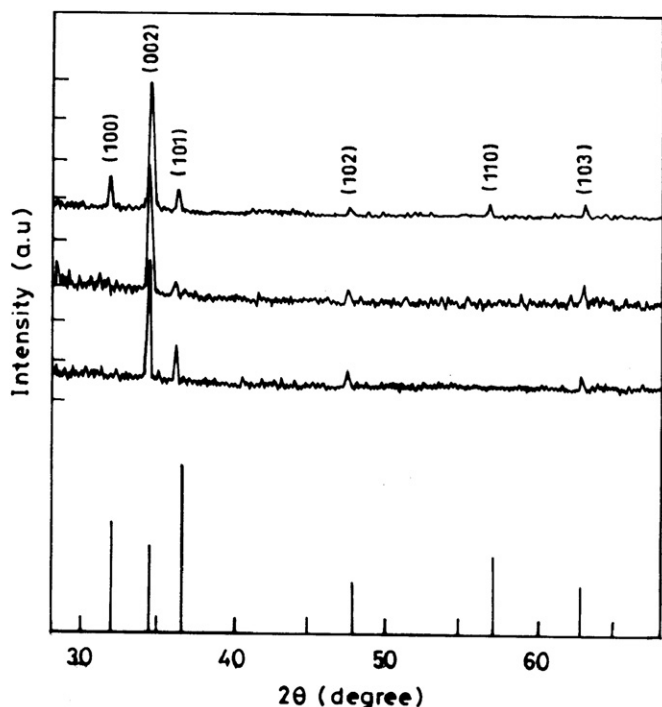

Fig. 1. X-ray diffraction patterns of the ZnO films formed by heating at different temperatures: (a) 400 (b) 450 and (c) 500 °C.

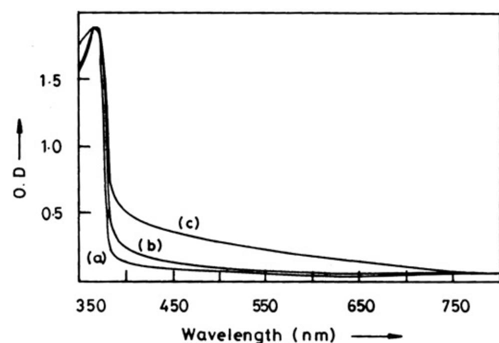

Fig. 2. Absorbance spectra of the ZnO films formed by heating at different temperatures: (a) 400 °C (b) 450 °C and (c) 500 °C.

500 °C. It was observed that as the post heat treatment temperature increases, the intensity of the (1 0 0) peak increases and the width of the (0 0 2) peak decreases. For the samples heated at 500 °C, the FWHM of the (0 0 2) peak was 0.194, while for the samples heated at 450 and 400 °C, the FWHM of the (0 0 2) peak were 0.241 and 0.274, respectively. This may be due to the fact that low temperatures lead to formation of smaller grains compared to high temperatures.

UV–vis absorption experiments were performed using a Hitachi U3400 UV–vis–NIR spectrophotometer. Fig. 2 shows the UV–vis absorption spectra of the samples heat treated at different temperatures. Films heat treated at temperatures greater than 400 °C show greater absorption at longer wavelengths. The tail height increases as the heat treatment temperature increases. The tail may be caused by an enhanced scattering effect of the smaller ZnO grains. The increase of the FWHM value of the (0 0 2) XRD peak for the samples heated at temperatures less than or equal to 450 °C is an additional, strong evidence for smaller grain size.

Fig. 3 shows the morphology of films heat treated at different temperatures studied using a JEOL SEM attached with energy dispersive X-ray (EDX) system. It is apparent from the electron micrographs that the morphology is strongly dependent on the temperature of heat treatment. A granular and rounded grain growth is observed in all the cases. In fact, for the films heat treated at 400 °C, particle size is of the order of 50 nm (Fig. 3a), which is uniformly distributed giving a smooth surface morphology. As the heat treatment temperature increases to 450 °C, an apparent agglomeration of very small grains occurs, as is seen in Fig. 3b. The average diameter in this case is about 100 nm. Finally, well-defined grains, many of them hexagonal-shaped, with an average grain size of 150 nm is observed for the films heat treated at 500 °C (Fig. 3c).

The composition of ZnO films heat treated at 500 °C was analyzed by EDX measurement as shown in Fig. 4. The

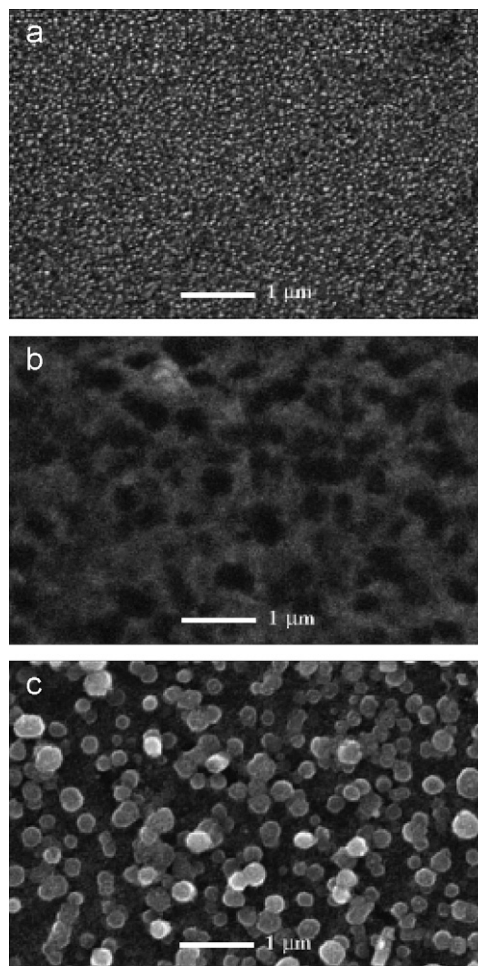

Fig. 3. Scanning electron micrographs of the ZnO films formed by heating at different temperatures: (a) 400 °C (b) 450 °C and (c) 500 °C.

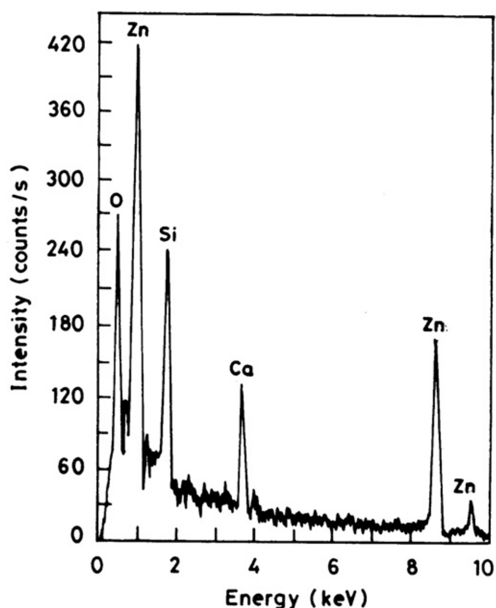

Fig. 4. EDX spectrum of the ZnO films formed by heating at 500 °C.

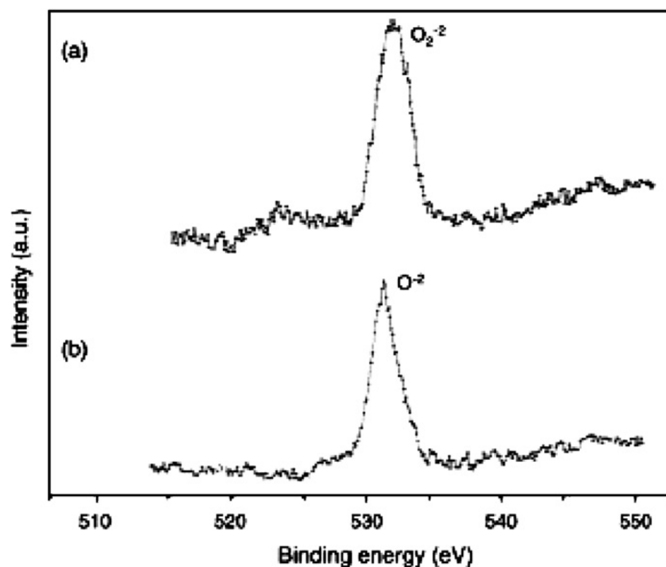

Fig. 5. XPS spectra of O levels of the ZnO films formed by heating at different temperatures: (a) 450 °C and (b) 500 °C.

EDX analysis shows that zinc, oxygen, silicon and calcium are present. The latter two come from the glass substrate.

XPS spectrum of the ZnO films heat treated at 500 °C was measured using MKIII Vac generators XPS system with Mg K_{α}. Figs. 5a and b reveal the O1s core level of ZnO before and after heat treatment at 500 °C. The spectrum shows peak at 533 eV (before) and 532.1 eV (after), which is attributed to O_2^{2-} and O^{2-} species, respectively. This result is in close agreement with the literature values [20]. Figs. 6a and b show Zn2p level spectrum of ZnO before and after heat treatment at 500 °C. The spectrum reveals the spin–orbit splitting of $Zn2p_{3/2}$

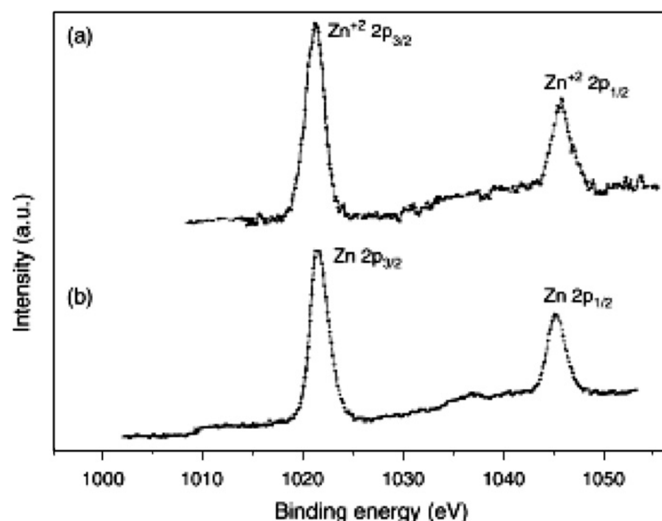

Fig. 6. XPS spectra of Zn levels of the ZnO films formed by heating at different temperatures: (a) 450 °C and (b) 500 °C.

ground state to be 1022.5 eV while the $Zn2p_{1/2}$ excited state is observed at 1045.7 which is attributed to Zn^{+2} in ZnO. Consequently, peaks at 1022.5 and 1045.5 eV correspond to $Zn2p_{3/2}$ (ground state) and $Zn2p_{1/2}$ (excited state), respectively.

The resistivity of ZnO films annealed from 400 to 500 °C was measured by providing Au contacts at the edges of the films. The results show that the resistivity increases from 1000 to 10,000 ohm cm with increasing heat treatment temperature. The probable reason is that the concentration of interstitial Zn decreases with increasing annealing temperature, because of Zn evaporation. ZnO contains vacancies within the crystal structure, and it can accommodate interstitial atoms easily [21]. The Zn interstitial atoms are easily ionized, and electrons produced by the ionized Zn interstitial atoms have large contribution to electrical conductivity. To decrease the resistivity, the films have to be doped with impurities like Al, Ga, etc. [22,23].

4. Conclusions

The results of this investigation clearly demonstrate the possibility of depositing ZnO films possessing reasonable resistivity and band gap which are comparable with the earlier reports. The resistivity can be brought down by doping with impurities like Ga, Al, Mn, etc. Further work is planned towards achieving this.

References

[1] P. Mitra, A.P. Chatterjee, H.S. Maiti, Mater. Lett. 35 (1998) 33.
[2] C.H. Kwon, H.K. Hong, D.H. Yun, K. Lee, S.T. Kim, Y.H. Roh, B.H. Lee, Sens. Actuators B 25 (1995) 610.
[3] K.L. Chopra, S. Major, D.K. Pandya, Thin Solid Films 102 (1983) 1.
[4] S. Major, A. Banerjee, K.L. Chopra, Thin Solid Films 143 (1986) 19.
[5] J.B. Yoo, A.L. Fahrenbruch, R.H. Bube, J. Appl. Phys. 68 (1990) 4694.
[6] D. Dimova-Malinovska, J. Lumin. 80 (1999) 207.

[7] Z.-C. Jin, I. Hamberg, C.G. Granqvist, B.E. Sernelius, K.-F. Berggren, Thin Solid Films 164 (1988) 381.
[8] J.G.E. Gardeniers, Z.M. Rittersma, G.J. Burger, J. Appl. Phys. 83 (1998) 7844.
[9] Y. Zhou, P.J. Kelly, A. Postill, O. Abu-Zeid, A.A. Alnajjar, Thin Solid Films 447–448 (2004) 33.
[10] G. Machado, D.N. Guerra, D. Leinen, J.R. Ramos-Barrado, R.E. Marotti, E.A. Dalchiele, Thin Solid Films 490 (2005) 124.
[11] Z.B. Shao, C.Y. Wang, S.D. Geng, X.D. Sun, S.J. Geng, J. Mater. Process. Technol. 178 (2006) 247.
[12] B.G. Choi, I.H. Kim, D.H. Kim, K.S. Lee, T.S. Lee, B. Cheong, Y.-J. Baik, W.M. Kim, J. Eur. Ceram. Soc. 25 (2005) 2161.
[13] P. Nunes, B. Fernandes, E. Fortunato, P. Vilarinho, R. Martins, Thin Solid Films 337 (1999) 176.
[14] C. Messaoudi, D. Sayah, M. Abd-Lefdil, Phys. Status Solidi (a) 151 (1995) 93.
[15] M. Krunks, E. Mellikov, Thin Solid Films 270 (1995) 33.
[16] D.J. Goyal, C. Agashe, M.G. Takwale, B.R. Marathe, V.G. Bhide, J. Mater. Sci. 27 (1992) 4705.
[17] M.A. Lucio-Lopez, M.A. Luna-Arias, A. Maldonado, M. de la L. Olvera, D.R. Acosta, Sol. Energy Mater. Sol. Cells 90 (2005) 733.
[18] D.F. Paraguay, L.W. Estrada, D.R. Acosta, M.E. Andrade, M. Yoshida, Thin Solid Films 350 (1999) 192.
[19] T. Mahalingam, V.S. John, M. Raja, Y.K. Su, P.J. Sebastian, Sol. Energy Mater. Sol. Cells 88 (2005) 227.
[20] C.D. Wagner (Ed.), Hand Book of X-Ray Photoelectron Spectroscopy, Perkin-Elmer, Minnesota, 1979.
[21] L.V. Azaroff, Introduction to Solids, McGraw-Hill, New York, 1960, pp. 371–372.
[22] J. Lee, D. Lee, D. Lim, K. Yang, Thin Solid Films 515 (2007) 6094.
[23] A.Kh. Abduev, A.K. Akhmedov, A.Sh. Asvarov, Sol. Energy Mater. Sol. Cells 91 (2007) 258.